Lab on a Chip

Miniaturisation for chemistry, biology & bioengineering

www.rsc.org/loc

Volume 8 | Number 8 | August 2008 | Pages 1229–1408

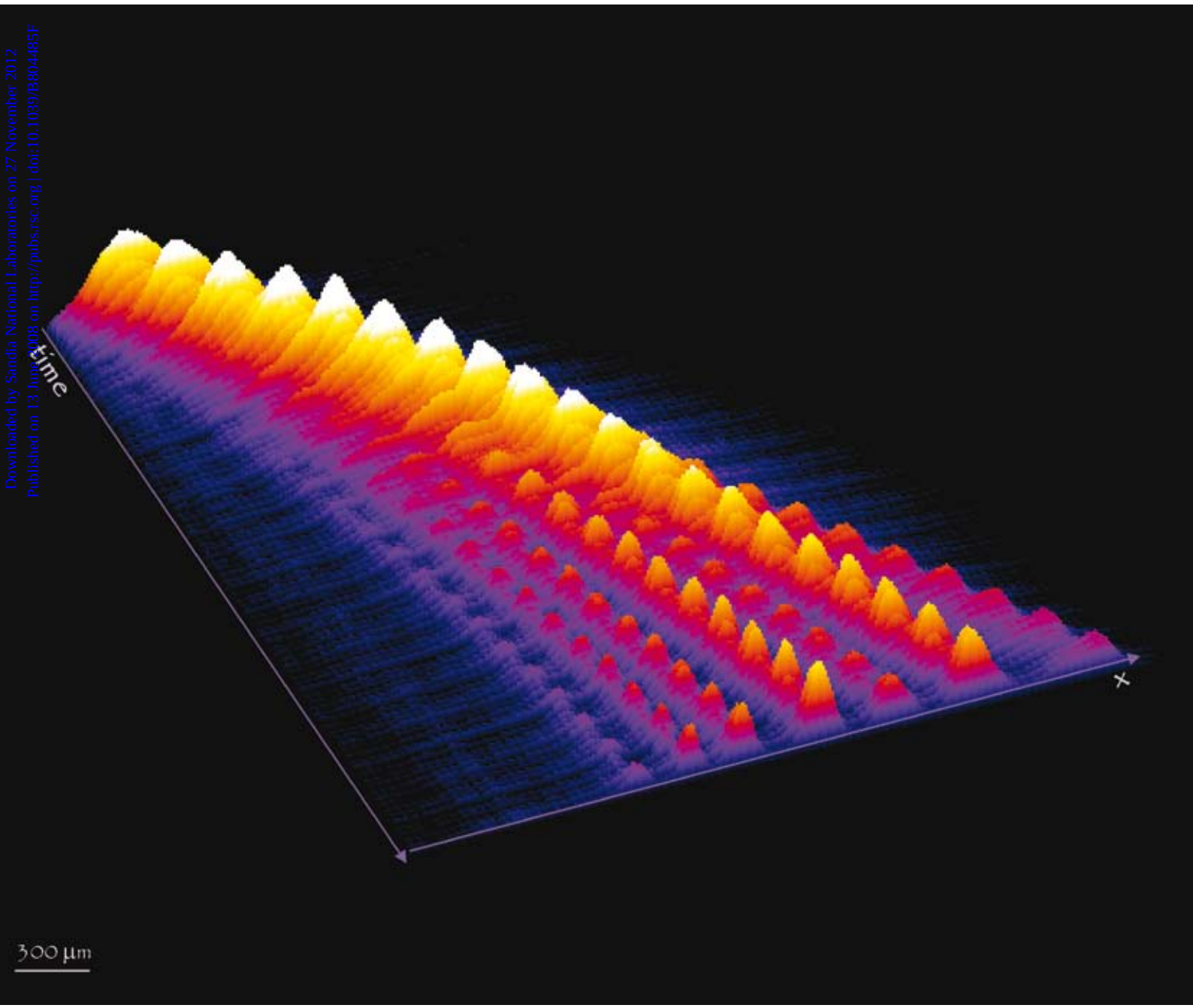

ISSN 1473-0197

RSC Publishing

Photopolymerized diffusion-defined polyacrylamide gradient gels for on-chip protein sizing

Catherine T. Lo,†[a] Daniel J. Throckmorton,†[b] Anup K. Singh[b] and Amy E. Herr*[c]

Received 17th March 2008, Accepted 8th May 2008
First published as an Advance Article on the web 13th June 2008
DOI: 10.1039/b804485f

We report on a facile diffusion-based photopatterning technique for generating linear and non-linear decreasing pore-size gradients in cross-linked polyacrylamide gels. Diffusion of low viscosity polymer precursor solutions and a two-step photopatterning process were used to define the decreasing pore-size gradient gels in a microfluidic format, thus eliminating the need for controlled mixing and delivery of polymer precursor solutions. We present an analytical model of the non-steady state diffusion process and numerically evaluate that model for direct comparison with empirical characterizations of the gradient gels. We show that the analytical model provides an effective means to predict the steepness and linearity of a desired gradient gel prior to fabrication. To assess electrophoretic assay performance in the microfluidic gradient gels, on-chip sizing of protein samples (20–116 kDa) was investigated. Baseline resolution of six proteins was demonstrated in 4 s using 3.5% to 10% polyacrylamide gradient gels. The demonstrated ability to conduct efficient protein sizing in ultra-short separation lengths (0.3 cm) means low applied electric potentials are needed to achieve the electric field strengths required for protein separations. The low required electric potentials relax operating constraints on electrical components, as is especially important for translation of the assay into pre-clinical and clinical settings. The gradient gel fabrication method reported is amenable to adaptation to non-sizing protein assays, as well as integration with upstream sample preparation steps and subsequent orthogonal downstream assays.

Introduction

For decades, continuous and discontinuous gradients in polyacrylamide gels have proven effective for high resolution protein sizing.[1–4] Especially important to the analysis of complex biological fluids consisting of protein components that span a wide molecular weight range,[5] gradient polyacrylamide gels are crucial to multi-dimensional separations that underpin advances in proteomics.[1] Over the last few decades, electrophoresis—both native and sizing—has benefited from significant advantages afforded through use of capillary and microfluidic formats. In particular, microchannel formats have reduced required analysis times, increased the potential for automation, and simplified integration complexity.[6] Protein sizing using matrices with uniform sieving properties has been successfully adapted for use in capillary[7–10] and microdevice formats.[11–14]

Fabrication of gel pore-size gradients in microanalytical systems has been achieved by mimicking approaches commonly used to fabricate macroscale slab gels;[15] that is, by controlling flow rate and filling duration of polymer precursor solutions loaded using dual syringe pumps (*i.e.*, gradient mixers).[16,17] A variation of the conventional gradient mixer approach used in slab gels was reported by Chen and Chang,[18] wherein electroosmotic flow was used to load polymer precursor solutions into microfluidic channels. Especially relevant to microsystems, both Liang *et al.*[16] and Chen and Chang[18] noted stringent fabrication demands on control of precursor flow rate and filling time, as the total volume of capillary and microdevice separation channels is quite small. Recent work described a modification of the mixer-based approach in a "step filling" and chemical polymerization method.[19] In this work, the authors 'dipped' the end of a capillary sequentially into fluid reservoirs, layering various polymer precursor compositions into the capillary column. A 5 h polymerization step followed and a step-like pore-size gradient was created in the capillary. The developers of the step filling approach noted that the fabrication technique suffers from multiple labor-intensive steps, yielding gel gradients with substantial capillary-to-capillary variation in spatial properties. Well-controlled micromachining processes (electrochemical etching) have also been reported as a means to generate pore-size gradients in porous silicon, with the gradient subsequently used to measure the size of bovine serum albumin.[20] Nevertheless, the reported fabrication technique is time-consuming and requires specialized instrumentation.

Adoption of pore-size gradient methods in capillary systems and microdevices has been hampered by the exceptional

[a]*Department of Biomedical Engineering, Yale University, New Haven, CT, USA*
[b]*Biosystems Research Department, Sandia National Laboratories, Livermore, CA, 94550, USA*
[c]*UCSF/UC Berkeley Joint Graduate Group in Bioengineering and Department of Bioengineering, University of California at Berkeley, Berkeley, CA, USA. E-mail: aeh@berkeley.edu*
† Both authors contributed equally to the work.

sensitivity of the resultant quality of the pore-size gradients on bulk fluid handling control, as well as by demands for specialized instrumentation. Interestingly, an early report by Ruchel[21] described fabrication of linear pore-size gradients using an elegant approach that relied on diffusion between two polyacrylamide precursor solutions introduced serially *via* suction into a capillary. After a reaction interval, chemical polymerization yielded 15 mm long pore-size gradients. As implemented by Ruchel and co-workers, well-understood diffusion processes are an attractive means to establish gel pore-size gradients in microscale systems.[21–23] Minimized reliance on bulk fluid handling for pore-size gradient generation potentially surmounts the aforementioned fabrication difficulties.

Building on the work of Ruchel and colleagues,[22] in combination with photolithographic fabrication techniques, we report on a diffusion-based fabrication method that readily yields linear and non-linear gradient gels in planar microfluidic devices. Empirical characterization of the gradients is presented, as is an analytical framing of the diffusion process that governs the axial profile of the acrylamide concentration (prior to photopolymerization) and the resulting polyacrylamide pore-size gradient (post-photopolymerization). Both non-steady state and steady state design rules are described to aid in the development of gradient gels having a variety of axial pore-size distributions for applications including protein sizing. To illustrate the power of the described on-chip gradient gels, we report on protein sizing of a mixture of proteins spanning a wide molecular weight range (20.1–116 kDa) in ultra-short separation lengths (0.3 cm)—an analysis demonstrated to require less than 4 s. Major advantages of the fabrication approach include ready integration of customizable gels with on-chip sample filtering and enrichment methods,[24,25] as well as eventual inclusion of optimized gradient gels in automated multi-dimensional assays.

Experimental

Chemicals

The water-soluble photoinitiator 2,2′-azobis[2-methyl-*N*-(2-hydroxyethyl)propionamide] (VA-086) was purchased from Wako Chemicals (Richmond, VA). Solutions of 3-(trimethoxysilyl)-propyl methacrylate (98%), 40% acrylamide (MW: 71.1), and 30% (37.5:1) acrylamide/bis-acrylamide were purchased from Sigma. Premixed 10× Tris–glycine–SDS (sodium dodecyl sulfate) electrophoresis buffer (25 mM Tris, pH 8.3, 192 mM glycine, 0.1% SDS) was purchased from BioRad (Hercules, CA). Deionized water (18.2 MΩ) was obtained using an Ultrapure water system from Millipore (Milford, MA).

Protein samples

Bovine serum albumin (BSA, MW 66k Da) was used as a protein tracer of known molecular weight (Sigma Aldrich, St. Louis, MO). Alexa Fluor 488 protein labeling kits were purchased from Molecular Probes (Invitrogen, Carlsbad, CA). BSA was fluorescently labeled with Alexa Fluor 488 per instructions provided in the product information accompanying the fluorescent labeling kit. A high molecular weight ladder, consisting of six fluorescently labeled species in solution (62 mM Tris, 1 mM EDTA, 3% sucrose, 0.5% dithiothreitol, 2% SDS and 0.005% bromophenol blue) was purchased from Sigma. The markers included: trypsin inhibitor (soybean), MW 20.1 kDa; carbonic anhydrase (bovine erythrocyte), 29 kDa; alcohol dehydrogenase (horse liver), 39.8 kDa; albumin (bovine serum), 66 kDa; β-galactosidases (*E. coli*), 116 kDa; and myosin (rabbit muscle), 205 kDa. In most sizing assays, myosin was found to yield a poor signal-to-noise ratio. All fluorescently labeled species were stored at 4 °C in the dark until use. Proteins were prepared for sizing per instructions from the supplier. Protein samples were denatured by mixing 2 : 1 with denaturing buffer (4% SDS and 3% β-mercaptoethanol) and heating to 85 °C for 3 min. Note that the absolute concentration of each protein in the stock solution was unknown. Post-labeled protein concentrations analyzed through fluorescence imaging were estimated to be in the low micromolar range.

Chip fabrication and fluidic interface

Quartz microfluidic chips were designed in-house and fabricated using standard wet etch processes by Caliper Life Sciences (Hopkinton, MA). The chips used for protein sizing consisted of offset double-T junctions having a separation channel that measured 3.8 cm in length. The channels were ~40 μm deep × ~100 μm wide. Fluidic interfacing to the chip employed a Delrin® fluidic manifold with fasteners clamping an aluminium frame so as to sandwich the fluidic chip.[26] O-rings were used to fluidically seal the polymer manifold against the glass chip. Fluid reservoirs were open to the ambient atmosphere and contained 100 μL of buffer or sample.

Channel surface

As in our previous work,[27–29] microchannels were prepared for polyacrylamide gel polymerization by functionalizing the channel surfaces with an acrylate-terminated self-assembled monolayer. The acrylate monolayer was formed using a 2 : 3 : 5 ratio mixture of 3-(trimethoxysilyl)propyl methacrylate, glacial acetic acid, and deionized water. The mixture was agitated vigorously (during water addition) and sonicated under vacuum for 5 min. Unwetted channels were filled with the acrylate mixture *via* capillary action. At the end of a 30 min static incubation step, the surface preparation solution was vacuum purged from all channels.

Gel precursor

Polyacrylamide gels of various acrylamide concentrations were fabricated in the microdevices. The concentration of acrylamide monomer and bis-acrylamide cross-linker determines the pore size of the gel. The concentration of total monomer is denoted by %T, while the proportion of cross-linker (as a percentage of total monomer) is denoted by %C. Generally, the higher the acrylamide concentration, the smaller the pore size of the final gel. Several *n*%T (n = 3.5, 6, and 10; all gels had 2.5%C; thus, hereafter references to "%T" will omit the "T") polyacrylamide gel matrices were fabricated by adjusting the total volume of the 30% acrylamide/bis-acrylamide solution. The final volume was adjusted with Tris-glycine–SDS run buffer containing 0.2% (w/v) VA-086 photoinitiator to achieve a (30/n)-fold dilution of acrylamide/bis-acrylamide. The gel precursor solutions were

exhaustively degassed (3–5 min under vacuum while sonicated) just prior to loading into the microchannels. (Note: Acrylamide is a neurotoxin absorbed through the skin. Proper handling and disposal procedures are required.) The gradient gel fabrication process is described in the Results and discussion section.

Apparatus and imaging

Electrophoretic transport was used to mobilize species, as all channels contained cross-linked polyacrylamide at the end of the fabrication process (see Fig. 1). The sample (S), sample waste (SW), buffer (B), and buffer waste (BW) reservoirs are indicated in Fig. 1. Prior to sizing, the sample reservoir was filled with the sample solution. A programmable high-voltage power supply provided voltage control and current monitoring through platinum electrodes.[26] Samples were loaded by applying a +700 V potential at the SW reservoir and grounding the S reservoir for ~1 min (E = 700 V cm^{-1}). During loading, both the B and BW reservoirs were grounded to form a well-defined 'pinched' injection plug. During the sizing separation, a +1112 V potential was applied at the BW reservoir while grounding the B reservoir (E = 298 V cm^{-1}). Chips having either a gradient or single percentage gel were used to analyze multiple sample mixtures with little to no observable retained fluorescence. To assure minimal cross-contamination between samples, all channels were electrophoretically flushed with buffer prior to storage.

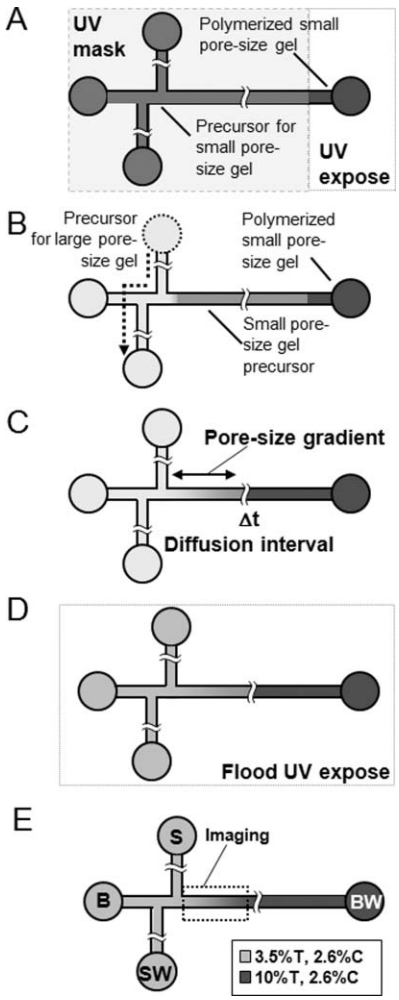

Fig. 1 Acrylamide diffusion defines gel pore-size gradient for on-chip protein sizing. Fabrication steps include: (A) all channels are filled with high total acrylamide concentration gel precursor solution, (B) masking and UV exposure define small pore-size gel plug at terminus of separation channel, (C) flushing exchanges non-polymerized high total acrylamide gel precursor with low total acrylamide concentration gel precursor solution in loading channels and at junction-region, (D) diffusion of precursor solutions occurs during a set diffusion period (Δt_m), (E) entire device is subjected to flood UV exposure, resulting in photopolymerization of both low and high total acrylamide gel precursor solutions and definition of the pore-size gradient. The process results in cross-linked polyacrylamide throughout the device.

A 1300 × 1030 Peltier-cooled interline CCD camera (CoolSnap HQ, Roper Scientific, Trenton NJ) was employed to monitor protein migration into and along the channels. Pixel binning (2 × 2) and region of interest selection were employed, thus allowing an image-sampling rate of greater than 10 Hz. A 0.31× de-magnifier (Diagnostic Instruments Inc., Sterling Heights, MI) was used to increase the field of view projected onto the CCD. Images were collected using an inverted epi-fluorescence microscope (IX-70, Olympus, Melville, NY) equipped with 4× objective (numerical aperture of 0.16). An x–y translation stage (Olympus, Melville, NY) was used to position the chip and fixturing relative to the imaging optics.

Data analysis

Image analysis was completed using ImageJ (http://rsb.info.nih.gov/ij/).[30] All images were background subtracted to correct for background signal. Numerical evaluations were carried out using Mathcad 2001i (Parametric Technology Corporation, Needham, MA).

Results and discussion

Fabrication of gradient gels for protein sizing

Gradient gels having varied characteristics (*e.g.*, steepness, gel pore-size boundary conditions, and shape) were designed using a diffusion-based method combined with photopolymerization processes. Sizing gels were fabricated so as to transition from large to small pore-size along the separation channel (*i.e.*, decreasing pore-size gels). Fig. 2 schematically depicts gradient gel characteristics as a function of location, L, along the separation channel. Three canonical gradient gels are illustrated in Fig. 2 and characterized in this work: (i) a uniform pore-size gel (a "single percentage" gel of acrylamide concentration C_1), (ii) a non-linear pore-size gradient varying from large pore-size (acrylamide concentration C_1) to small pore-size gel (acrylamide concentration C_2), and (iii) a linear gradient gel between acrylamide concentrations C_1 and C_2. Single percentage polyacrylamide gels were fabricated by loading the gel precursor solution into all microchannels, followed by a 15 min flood UV photopolymerization as described previously by our group.[27]

Devices were designed such that the final gradient gels consisted of a large pore-size loading gel, a pore-size gradient region along the separation axis, and a final small pore-size gel at the separation channel terminus (Fig. 1). First, to define and localize the smaller pore-size gel at the terminating end

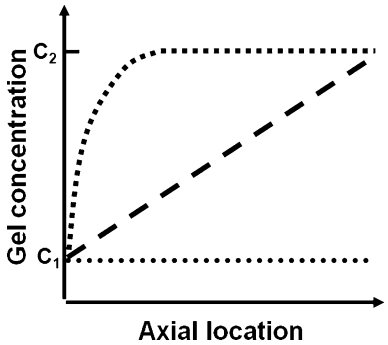

Fig. 2 Canonical acrylamide concentration profiles relevant to on-chip protein sizing. Gel concentration profiles along the separation axis of a microchannel can be described as: uniform acrylamide concentration C_1 (single percentage gels), non-linear increasing (or decreasing) acrylamide concentration variation from C_1 to C_2, and linear acrylamide concentration variation from C_1 to C_2.

of the separation channel (Fig. 1A), all channels were loaded with the high percentage acrylamide gel precursor solution *via* capillary action. The high percentage acrylamide gel precursor solution consisted of degassed 10% (37.5 : 1) acrylamide/bis-acrylamide containing 0.2% (*w*/*v*) VA-086 in 1× Tris–glycine–SDS buffer. A gel plug was fabricated at the outlet of the separation channel *via* photomasking and a 10 min flood UV exposure using a fan-cooled 100 W lamp (Fig. 1A). Fabrication of the plug resulted in: (i) a separation channel filled with the high percentage acrylamide gel precursor solution and (ii) no bulk flow in the horizontal separation channel. Next, to define the larger pore-size gel establishing the separation channel inlet boundary condition the low percentage acrylamide gel precursor solution was pressure-filled *via* a syringe into the loading channels (Fig. 1B). The loading gel precursor solution consisted of degassed 3.5% (37.5 : 1) acrylamide/bis-acrylamide containing 0.2% (*w*/*v*) VA-086 in 1× Tris–glycine–SDS buffer.

A defined "diffusion interval" (denoted by Δt_m, where *m* represents the duration of the diffusion interval in minutes) was implemented to establish the axial gradient in acrylamide concentration (Fig. 1C). During this time period, both the low and high percentage acrylamide gel precursor solutions were near-quiescent. As mentioned, bulk flow was eliminated in the plug-capped separation channel. Finally, at the end of the diffusion period, photopolymerization of both gel precursor solutions was conducted *via* a 15 min photopolymerization of the unmasked chip using a 100 W 355 nm lamp (Fig. 1D). Diffusion intervals spanning from 0 min (Δt_0) to 120 min (Δt_{120}) were employed. As will be described, the range of diffusion intervals explored in this work yielded gradient gels with separation lengths of less than 1 cm. After fabrication and when not in use, chips were stored wetted and submerged in buffer at 4 °C. The yield of fabricated gels was ~90%. Once successfully fabricated, chip usage lifetimes typically exceeded 20+ hours of usage per week over several weeks.

Uniform gels for electrophoretic mobility calibration

As a means to calibrate the pore-size distribution in gradient gels, the apparent mobility of a fluorescent scalar (BSA) was measured in single percentage gels having a uniform, known composition. Three single percentage polyacrylamide gels (3.5%, 6%, 10%; all with 2.5%C) were used to calibrate the dependence of the apparent mobility of the scalar on gel composition. Calibration of the tracer mobility yielded the following linear dependence of mobility on gel composition: $\log(\text{mobility, cm}^2\ \text{V}^{-1}\ \text{s}^{-1}) = -0.114\,(\%n) - 3.16\ (R^2 = 0.998)$, where $\%n$ indicates the acrylamide composition of the calibration gel (*e.g.*, 3.5%, 6%, and 10%). The measured relationship between protein mobility and total acrylamide concentration is as expected from theory.[31]

Characterization of gradient gels having non-uniform sieving properties

Protein sizing gels with gradients ranging from 3.5% (C_1, at the injection junction of the separation channel) to 10% (C_2, at the end of the separation channel) were fabricated. To characterize the spatial sieving qualities of the on-chip gradient gels, location-dependent apparent mobility of the tracer peak was extracted from CCD observations of the location-dependent velocity of the tracer peak and known electric field. Fig. 3 shows the observed mobility of the tracer peak as a function of axial location (distance from the injection junction) for three 3.5% to 10% gradient sizing gels–each fabricated with a different diffusion interval, in this case: 0 min (Δt_0), 30 min (Δt_{30}), and 120 min (Δt_{120}).

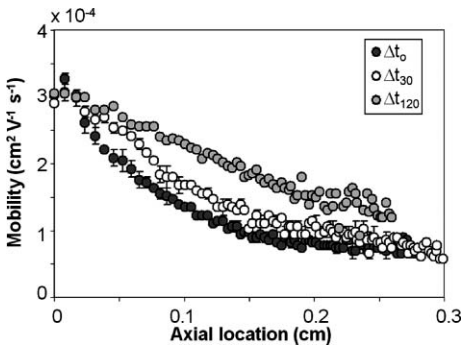

Fig. 3 Full-field imaging allows extraction of protein tracer mobility as a function of axial location for various on-chip sizing gels. Diffusion intervals examined include: (i) Δt_0: minimal time was allowed between flushing of 3.5% gel precursor solution and flood UV photopolymerization of gradient gel, (ii) Δt_{30}: a diffusion period of 30 minutes, and (iii) Δt_{120}: a diffusion period of 120 minutes. $E = 298$ V cm^{-1}.

As can be observed from Fig. 3, the tracer exhibits the same mobility during the initial injection (3.5% gel portion) in all three sizing gels. This initial 3.5% portion of the gel essentially acts as a 'loading gel'—a large pore size gel that minimizes molecular weight-related sample injection bias during loading. As the tracer electrophoreses away from the injection junction and into the separation gel along the separation channel, the apparent mobility is noticeably reduced owing to a decrease in the pore-size of the gel. Fig. 3 also illustrates the effect of the diffusion interval on the migration behavior of the tracer—the gradient gels defined by the Δt_0 and Δt_{30} diffusion intervals yield a markedly steeper reduction of the tracer mobility than the gel fabricated with the longer (Δt_{120}) diffusion interval, as anticipated.

Through calibration of the electrophoretic mobility of the tracer (Fig. 3) and the known gel composition, the axial pore-size gradient for each 'diffusion interval' was determined and is shown in Fig. 4. The Δt_0 gel exhibits an axial pore-size distribution that can be interpreted as a separation system comprised of a 'loading gel' (3.5% at injector) and a 'separation gel' (10% along the majority of the separation channel). In the case of the longer duration diffusion intervals (represented here by Δt_{120}), we observe a near-linear decrease in the effective pore-size of the gel. As has been described elsewhere, the high separation performance afforded by gradient gels is attributable to the polyacrylamide gel acting as a spatially-varying molecular sieve.[32] In a continuous gradient gel, such as commonly used in slab gels, proteins are electrophoretically-driven through progressively smaller pores. As a protein band migrates through the gradient gel, the molecular sieve differentially retards proteins according to size. Customization of the gradient gel shape (axially, along the separation channel) and composition yields readily tunable separation performance. While protein sizing assays benefit from decreasing pore-size gels, native electrophoretic assays may also benefit. Based on our previous work with homogeneous electrophoretic immunoassays in single percentage polyacrylamide gels (*i.e.*, uniform pore-size along separation axis),[28,29] we posit that use of a decreasing pore-size gel may aid in optimizing the separation of native immunecomplex from an associated probe (either antibody or antigen). Such optimization could even further reduce separation times for polyacrylamide gel-based electrophoretic immunoassays.

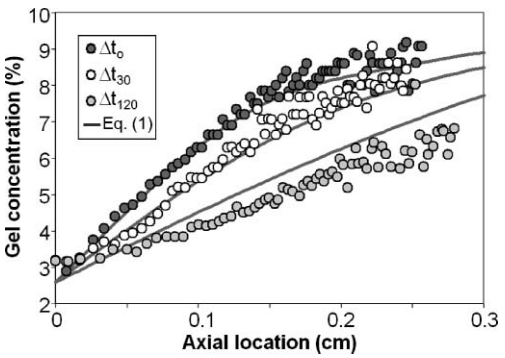

Fig. 4 Empirical characterization and numerical modeling of pore-size gradient linearity, as determined by the diffusion interval used during fabrication. Based on a calibrated relationship between the apparent electrophoretic mobility of the tracer (shown in Fig. 3) and the known gel precursor composition, the effective gel concentration can be estimated along the separation axis of the microchannel. Numerical evaluations of the non-steady state diffusion process used to define the gels are plotted as solid lines for each of the three gel types shown.

Comparing two chips fabricated on different days by different operators allowed an estimate of the chip-to-chip fabrication reproducibility. Here, we utilized measurements of BSA mobility as a function of distance along the separation axis. For gradient gels with no diffusion interval (Δt_0), less than 10% variation in measured average mobility values was measured at axial locations greater than 480 μm from the injection junction (480 μm $< x <$ 3600 μm). Near the injection junction (0 μm $< x <$ 480 μm), a 16% variation in measured average mobility was observed. For gradient gels fabricated with long diffusion intervals (*e.g.*, Δt_{120}), we observed 10–15% variation in measured mobility values at locations between the injection junction and 480 μm (*i.e.*, 0 μm $< x <$ 480 μm). At axial locations greater than 480 μm from the injection junction (480 μm $< x <$ 3600 μm), we observed less than 10% variation in measured average mobility values. For a single chip, run-to-run variation in measured average mobility values was less than 10% ($n =$ 7 runs) for each measured location along the separation axis. As compared to fabrication methods that rely on external control of mixing of two gel precursor solutions,[16] the diffusion-defined method reported here provides a robust, straightforward means to reproducibly generate pore-size gradients. Further, the reported method requires minimal sample handling control (*i.e.*, volumetric flow rate or mixing control needed when using a conventional or microfluidic gradient mixer).

Design of gradient gel

To characterize and predict the impact of the diffusion interval on the shape of the pore-size gradient, the solution to non-steady state diffusion in one-dimension (without advection) was evaluated numerically for the boundary conditions, initial condition, and axial range of interest: $c(0, t) = C_1$ and $c(L, t) = C_2$ for all $t \geq 0$; $c(x, 0) = f(x)$ for $0 \leq x \leq L$. Where $c(x,t)$ describes the effective total acrylamide concentration of the gel, C_1 and C_2 are constants describing the boundary acrylamide concentrations, $f(x)$ is an empirically-determined function describing the initial condition, x is the axial location along the separation channel, and t is time.

Based on the empirically-determined gradient gel properties, the boundary condition C_1 was estimated to be 2.6%, less than the desired 3.5% loading gel concentration. The observed C_1 boundary condition at the injection junction is attributed to fabrication variation and measurement error in the mobility near the injection junction. For numerical evaluation, the gel concentration C_2 was set at 10% for L much larger than the imaged area of the separation channel ($L >> 0.3$ cm). A least-square fit of an error function to the gradient gel formed with no diffusion interval (Δt_0) was used to generate the function, $f(x)$, defining the initial condition. The initial condition can be described as: $f(x) = c_0 \times \mathrm{erf}(\frac{x}{\sqrt{c_1}}) + c_2$ with $c_0 = 6.3$; $c_1 = 0.03$; and $c_2 = 2.6$. Dirichlet (or first type) boundary conditions were imposed on the geometry, such that gel composition was fixed as $C_1 = 2.6\%$ and $C_2 = 10\%$, to match the empirical data. The non-steady state solution for the final effective gel concentration can be obtained using separation of variables[33] and expressed as:

$$C(x,t) = C_1 + (C_2 - C_1)\frac{x}{L} + \frac{2}{\pi}\sum_1^\infty \frac{C_2\cos n\pi - C_1}{n}\sin\frac{n\pi x}{L}\exp[-Dn^2\pi^2 t/L^2] + \frac{2}{L}\sum_1^\infty \sin\frac{n\pi x}{L}\exp[-D\pi^2 n^2 t/L^2]\int_0^1 f(x')\sin\frac{n\pi x'}{L}\mathrm{d}x' \quad (1)$$

Where D is the diffusion coefficient of aqueous acrylamide monomer (estimated at $D = 4 \times 10^{-6}$ cm^2 s^{-1}) and was employed as a fitting parameter. Eqn (1) describes the time and

location dependent acrylamide monomer concentration prior to photopolymerization. Numerical evaluations of Eqn (1) for each of the three diffusion intervals considered (Δt_0, Δt_{30}, Δt_{120}) are plotted with the empirical results in Fig. 4. Appreciable agreement between the shape and steepness of the empirically characterized gradient gel and the predicted gradient gel for diffusion intervals of Δt_{30} and Δt_{120} is observed. In the limit of steady-state, the relationship $t \sim (L)^2/2D$ can be used to estimate the time required to establish an acrylamide concentration gradient over a given separation length, L. For the gradient gels described in this work, the separation length employed was an ultra-short 0.3 cm. The steady-state limit indicates that a diffusion interval of 11 280 s (just over 3 h) is necessary to establish a linear gradient along L for the chip design used in this work.

Protein sizing of wide molecular weight range proteins using gradient gels

To assess the performance of the various gradient sizing gels, sizing of a sample of known proteins was performed. Five proteins, ranging in molecular weight from 20 kDa to 116 kDa were analyzed in 3.5% to 10% gradient gels. The model protein mixture was sized using both non-linear (Δt_0) and linear (Δt_{120}) gradient gels (Fig. 5). As noted, the decreasing pore-size gel starts (near the injection junction) with a large pore-size gel of 3.5% and decreases to a much smaller pore-size expected from a 10% gel. The fluorescence microscopy image montage presented in Fig. 5 show the non-linear decrease in electrophoretic mobility during sizing in a non-linear gel (Δt_0). In contrast, proteins migrate with a linear decrease in mobility in the linear pore-size gradient (Δt_{120}). Performance of the sizing assays was assessed using separation resolution (SR) for the largest two proteins in the molecular weight ladder (*i.e.*, alcohol dehydrogenase and bovine serum albumin). By four seconds into the sizing separation, the SR value of the linear gel (Δt_{120}) is nearly 50% better than the SR of the non-linear gel (Δt_0). As the separation progresses, the SR for both the linear and the non-linear gradient gels steadily increase. The SR for the linear gradient is nearly 50% higher than that observed for the non-linear gradient over the duration of the separation.

In a decreasing pore-size gradient the advancing edge of the migrating protein band is retarded preferentially, as compared to the trailing edge of the band. The well-known compression phenomenon results in substantial sharpening of protein bands and appreciable separation resolution.[1] As a means to illustrate the performance advantages of gradient gel sizing on separation performance, band variance (σ^2), as a function of migration distance (x), was compared for the protein tracer (BSA*) in a 6% single percentage gel and in the linear (Δt_{120}) 3.5% to 10% gel. The gradient gel provided plate heights ($H = \sigma^2/x$) that were substantially lower than the single percentage gel, for all times measured. After 6 s of electrophoresis, the plate height from the gradient gel was 1.40 μm, while the 6% gel yielded a 3.62 μm plate height, a 3.6-fold difference. For this case, we observe an appreciable separation performance improvement available from sizing using a linear gradient gel.

Given a reasonable long-time diffusion interval, we can employ the steady-state relationship described previously ($t \sim (L)^2/2D$) to estimate the axial length of a practically-achievable linear gradient. For the purposes of this illustration, we choose a practical diffusion interval of 15 h (overnight). The overnight diffusion interval would yield a linear polyacrylamide pore-size gradient over a 0.66 cm separation length. As demonstrated in this work, a 3.5% to 10% total acrylamide gradient gel spanning a 0.3 cm separation length is sufficient to

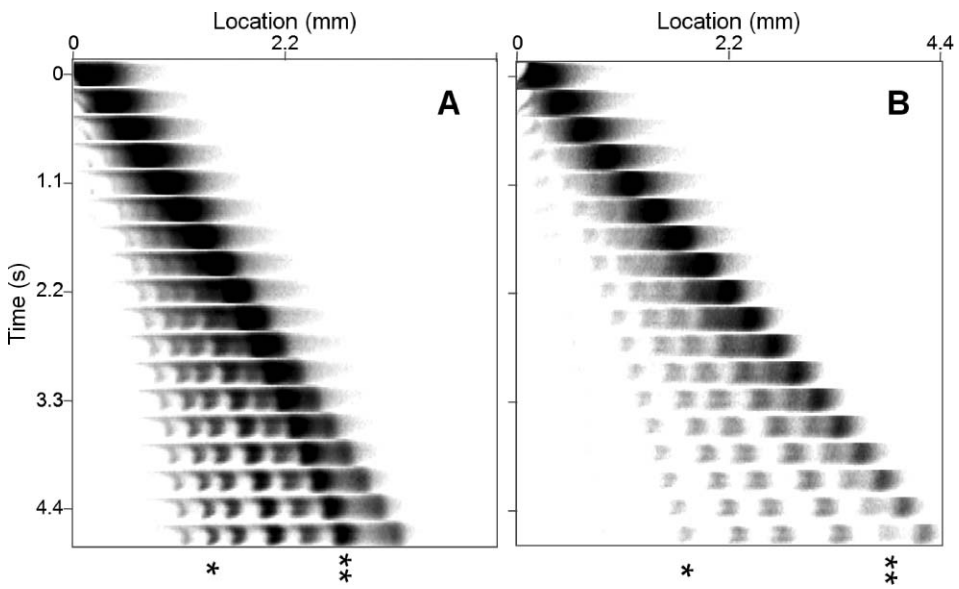

Fig. 5 Rapid sizing of proteins in ultra-short non-linear (Δt_0) and linear (Δt_{120}) decreasing pore-size gradient gels. (A) Note the non-linear decrease in protein mobilities in the Δt_0 gel visible in the inverted grayscale CCD images. (B) The non-linear behavior is not observed in the linear gradient gel. For visual reference, β-galactosidase (*) and trypsin inhibitor (**) are marked with asterisks at the bottom of each panel. Axial length of imaged channel is 4400 μm, channel width is 100 μm. $E = 298$ V cm^{-1}.

resolve species over a 20.1 to 116 kDa range. Given an overnight diffusion interval, we could expect to extend the molecular weight range of resolvable species even further by providing nearly double the separation length.

A systems design implication of the results shown in Fig. 5 regards the ability to conduct efficient protein sizing in ultra-short separation lengths with applied electric field strengths of 298 V cm^{-1}. In the chip geometry reported here, only a fraction of the total channel length (< 10%) was used for gradient gel-based sizing. Consequently, future chip designs will be implemented with significantly shorter total channel lengths of ~0.3 cm to ~1 cm. Accordingly, the electric potential required to provide 298 V cm^{-1} for sizing in the ultra-short separation channels will also be reduced. While the present geometry requires ~1 kV to achieve 298 V cm^{-1}, a design utilizing ultra-short total channel lengths would require applied electric potentials of 89 V to 298 V for 0.3 cm to 1 cm long separation channels, respectively. Sizing in ultra-short total channel lengths with low applied potential operating conditions are presently under investigation. The low electric potential required to drive electrophoresis in the ultra-short channels would substantially impact the design requirements for point-of-care instruments; namely, obviating the need for expensive high voltage power supplies and switching components.

Summary and conclusions

The diffusion-based method described here for generating spatial gradients in effective total acrylamide concentration and, hence, gel pore-size in microfluidic format has been characterized empirically. Building on an analytical model for non-steady state diffusion of acrylamide monomer in an aqueous solution, we have developed design guidelines for fabricating gels with known pore-size gradient profiles along the separation channel. The resulting linear and non-linear gradient gels allow assay optimization for protein samples of interest—being especially relevant to complex samples. Beyond ease of fabrication, the reported gradient gel fabrication method offers several advantages for microfluidic electrophoresis. First, the potential for optimizing on-chip gel characteristics for specific multi-component samples is attractive, particularly for development of systems for quantitation of proteins in heterogeneous biological samples. Second, the capability to size samples composed of a wide range of molecular weight proteins in ultra-short separation lengths is notably advantageous for designs of multiplexed analyses performed in compact devices. Further, the ability to implement electrophoretic analyses with appreciable applied electric field strengths, yet with low electric potentials requirement, is without a doubt desirable for high throughput bioanalytical instrumentations designed for portable use (*e.g.* point-of-care diagnostics). To our knowledge, no such accessible method for creating on-chip cross-linked gel pore-size gradients has been reported. Our group is currently developing the reported gradient gels for inclusion in streamlined, multi-stage bioanalytical systems that integrate sample preparation with multi-dimensional on-chip analyses such as non-equilibrium (protein sizing, native) and equilibrium-based (isoelectric focusing) electrophoresis.

Acknowledgements

The authors thank Dr Joshua I. Molho and Mr James S. Brennan for helpful discussion and suggestions. This work was financially supported by Sandia Laboratory Directed Research and Development (LDRD) program. AEH thanks the University of California at Berkeley for additional financial support. Sandia is a multi-program laboratory operated by Sandia Corp., a Lockheed Martin Co., for the United States Department of Energy under Contract DE-AC04-94AL85000.

References

1 J. Margolis and K. G. Kenrick, *Nature*, 1967, **214**, 1334–1336.
2 G. L. Wright, K. B. Farrell and D. B. Roberts, *Clin. Chim. Acta*, 1971, **32**, 285–296.
3 J. Margolis and K. G. Kenrick, *Anal. Biochem.*, 1968, **25**, 347–362.
4 J. Margolis and K. G. Kenrick, *Biochem. Biophys. Res. Commun.*, 1967, **27**, 68.
5 D. Rodbard and A. Chrambach, *Anal. Biochem.*, 1971, **40**, 95–134.
6 D. J. Harrison, K. Fluri, K. Seiler, Z. H. Fan, C. S. Effenhauser and A. Manz, *Science*, 1993, **261**, 895–897.
7 A. S. Cohen and B. L. Karger, *J. Chromatogr.*, 1987, **397**, 409–417.
8 S. Hjerten, K. Elenbring, F. Kilar, J. L. Liao, A. J. C. Chen, C. J. Siebert and M. D. Zhu, *J. Chromatogr.*, 1987, **403**, 47–61.
9 M. D. Zhu, D. L. Hansen, S. Burd and F. Gannon, *J. Chromatogr.*, 1989, **480**, 311–319.
10 A. Widhalm, C. Schwer, D. Blaas and E. Kenndler, *J. Chromatogr.*, 1991, **549**, 1–2.
11 L. Bousse, S. Mouradian, A. Minalla, H. Yee, K. Williams and R. Dubrow, *Anal. Chem.*, 2001, **73**, 1207–1212.
12 S. Yao, D. S. Anex, W. B. Caldwell, D. W. Arnold, K. B. Smith and P. G. Schultz, *Proc. Natl. Acad. Sci. U. S. A.*, 1999, **96**, 5372–5377.
13 L. J. Jin, B. C. Giordano and J. P. Landers, *Anal. Chem.*, 2001, **15**, 4994–4999.
14 Y. Li, J. S. Buch, F. Rosenberger, D. L. DeVoe and C. S. Lee, *Anal. Chem.*, 2004, **76**, 742–748.
15 J. Margolis, *Anal Biochem*, 1969, **27**, 319–322.
16 D. H. Liang, L. G. Song, M. A. Quesada, Z. W. Tian, F. W. Studier and B. Chu, *Electrophoresis*, 2000, **21**, 3600–3608.
17 D. H. Liang and B. J. Chu, *Electrophoresis*, 2002, **23**, 2602–2609.
18 H. S. Chen and H. T. Chang, *J. Chromatogr. A.*, 1999, **853**, 337–347.
19 Y. Chen, F. L. Wang and U. Schwarz, *J. Chromatogr. A*, 1997, **772**, 129–135.
20 B. E. Collins, K. P. S. Dancil, G. Abbi and M. J. Sailor, *Adv. Funct. Mater.*, 2002, **12**, 187–191.
21 R. Ruchel, *J. Histochem. Cytochem.*, 1976, **24**, 773–791.
22 R. Ruchel, S. Mesecke, D. I. Wolfrum and V. Neuhoff, *Hoppe-Seyler's Z. Physiol. Chem.*, 1974, **355**, 997–1020.
23 R. Ruchel, *J. Chromatogr.*, 1977, **132**, 451–468.
24 A. V. Hatch, A. E. Herr, D. J. Throckmorton, J. S. Brennan and A. K. Singh, *Anal. Chem.*, 2006, **78**, 4976–4984.
25 S. Song, A. K. Singh and B. J. Kirby, *Anal. Chem.*, 2004, **76**, 4589–4592.
26 R. F. Renzi, J. Stamps, B. A. Horn, S. Ferko, V. A. VanderNoot, J. A. A. West, R. Crocker, B. Wiedenman, D. Yee and J. A. Fruetel, *Anal. Chem.*, 2005, **77**, 435–441.
27 A. E. Herr and A. K. Singh, *Anal. Chem.*, 2004, **76**, 4727–4733.
28 A. E. Herr, D. J. Throckmorton, A. A. Davenport and A. K. Singh, *Anal. Chem.*, 2005, **77**, 585–590.
29 A. E. Herr, A. V. Hatch, D. J. Throckmorton, H. M. Tran, J. S. Brennan, W. V. Giannobile and A. K. Singh, *Proc. Natl. Acad. Sci. U. S. A.*, 2007, **104**, 5268–5273.
30 M. D. Abramoff, P. J. Magalhaes and S. J. Ram, *Biophotonics International*, 2004, **11**, 36–41.
31 K. A. Ferguson, *Metabolism*, 1964, **13**, 985–1002.
32 L. Ornstein, *Ann. NY Acad. Sci.*, 1964, **121**, 321–349.
33 J. Crank, *The Mathematics of Diffusion*, Oxford University Press, New York, 1975.